Proceedings of Symposium on Ultrasonic Electronics, Vol. 36 (2015)
5-7 November, 2015

Complex vibration source consisted of two transducers with longitudinal and torsional vibration mode
縦とねじり振動モードの 2 つの振動子を用いた複合振動源

Takuya Asami† and Hikaru Miura (College of Science and Technology, Nihon Univ.)
淺見拓哉†，三浦 光（日大・理工）

1. Introduction

Ultrasonic welding is a cold metal welding method. Previous studies have demonstrated that ultrasonic welding improves the weld strength by applying two-dimensional stress to the welding target [1]. We have used the planar vibration locus to investigate the two-dimensional stress applied to the welding target during ultrasonic welding. We obtained the planar locus by using an ultrasonic longitudinal-torsional vibration source with diagonal slits to drive two frequencies [2].

We have developed a new ultrasonic longitudinal-torsional vibration source to vibrate the planar locus. This new vibration source has two transducers with longitudinal and torsional vibration modes. Here, we describe the properties of the new vibration source.

2. Ultrasonic Vibration Source

Figure 1 shows the ultrasonic complex vibration source, which consists of a bolt-clamped Langevin-type longitudinal vibration transducer (resonance frequency of 29.9 kHz, Honda Electronics Co., Ltd.), a uniform rod of A2017 with a diameter of 40 mm and a length of 164 mm, and a bolt-clamped Langevin-type torsional vibration transducer (resonance frequency of 18.8 kHz, NGK Spark Plug Co.,Ltd.).

The wave propagation speed of longitudinal vibration and torsional vibration are about 5000 and 3000 m/s, respectively for A2017. We match the wavelength by changing the resonance frequency. The resonance frequencies of the transducers are different; however, the propagation wavelengths of the transducers are the same. The length of the uniform rod is one wavelength of the longitudinal and torsional vibration. In addition, the uniform rod has an M3 hexagon bolt at x = 82 mm for measuring the vibration locus. The bolt is too small to affect the vibration source.

3. Free admittance loops

The free admittance loops of the ultrasonic complex vibration source were measured with the terminal voltage of both transducers fixed at 1 V (effective value). The measurement range of the driving frequency was the resonance frequency ±1.0 kHz of both transducers.

Figure 2 shows the measured free admittance loops of the ultrasonic complex vibration source, where the vertical axis represents the susceptance and horizontal axis represents the conductance. The resonance frequency, f_{0L}, the quality factor, Q, and the motional admittance, $|Y_{m0}|$, of the longitudinal vibration were 29.4 kHz, 515, and 2.7 mS, respectively. f_{0T}, Q and $|Y_{m0}|$ of the torsional vibration were 18.8 kHz, 647, and 21.4 mS, respectively. The resonance frequencies of the longitudinal and torsional vibration were the same as the resonance frequencies of the transducers. $|Y_{m0}|$ of the longitudinal vibration was low compared with the torsional vibration. $|Y_{m0}|$ could be improved by the coil. However, in this paper, we measured the characteristics of the vibration source without the coil.

4. Vibration distribution

The longitudinal-torsional vibration distributions of the uniform rod were measured. The

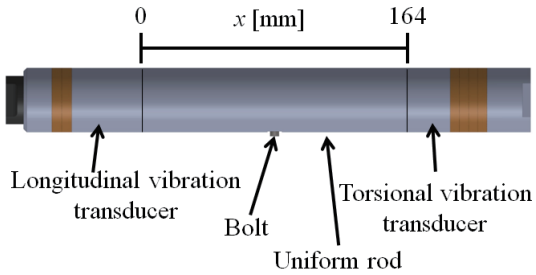

Fig. 1 Ultrasonic complex vibration source.

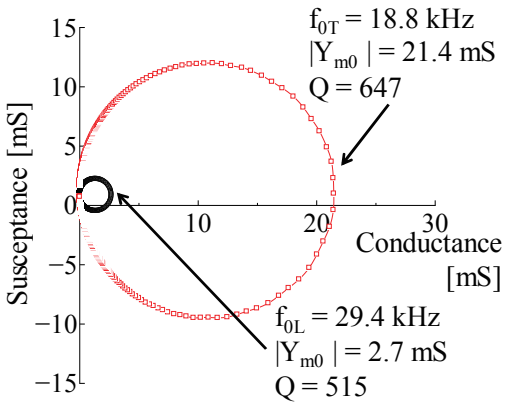

Fig. 2 Free admittance loops of the vibration source.

E-mail : asami.takuya@nihon-u.ac.jp†

longitudinal vibration displacement amplitude was measured by a ring-type magnetic ultrasonic vibration detector, and a laser Doppler vibrometer (LDV) was used to measure the torsional vibration displacement amplitude.

Figure 3 shows the longitudinal-torsional vibration distributions of the complex vibration source, where the vertical and horizontal axes represent the longitudinal or torsional vibration displacement amplitude normalized by the maximum vibration displacement amplitude and the measurement position in the x direction, respectively.

For the longitudinal and torsional vibration distributions, the resonance frequencies of both vibrations corresponded to the wavelength of the rod. The loop positions of both vibration displacement amplitudes were $x \approx 0$, 82, and 164 mm. The node positions of both vibration displacement amplitudes were $x \approx 41$ and 123 mm. The vibration distributions were similar; the slight change was caused by the nut on the longitudinal vibration transducer (left of Fig. 1). The diameter of the nut was smaller than the diameter of the uniform rod.

5. Vibration locus at the bolt

The vibration loci were plotted at each vibration resonance frequency. The longitudinal and torsional vibration displacement amplitudes of the M3 hexagon bolt were measured simultaneously with two LDVs at an input electric power of 1.0 W.

Figure 4 shows the vibration locus for the longitudinal-torsional vibration at the bolt. The vertical axis represents the torsional vibration amplitude and the horizontal axis represents the longitudinal vibration amplitude. Both vibration loci of each vibration resonance frequency were in a straight line in the direction of the longitudinal or torsional vibration. Next, based on these results, we measured the vibration locus while applying both resonance frequencies to the ultrasonic complex vibration source simultaneously. Furthermore, the experimental results in **Fig. 5** show that the vibration locus was rectangular planar. The rectangular planar locus was obtained as the sum of the straight loci of the two drive frequencies. These results indicate that the square planar locus was obtained by varying the input electric power.

6. Conclusions

In this study, the characteristics of our new ultrasonic longitudinal-torsional vibration source were determined. Both vibration distributions were consistent; thus, both vibration distributions were fixed simultaneously. The planar vibration locus was obtained. The results show that the new vibration source is suitable for ultrasonic welding.

References

1) J. Tsujino, et al.: Jpn. J. Appl. Phys. **46** (2007), pp. 4945-4947.
2) T. Asami and H. Miura : Acoust. Sci. & Tech. **36**, 3 (2015), pp. 232-239.

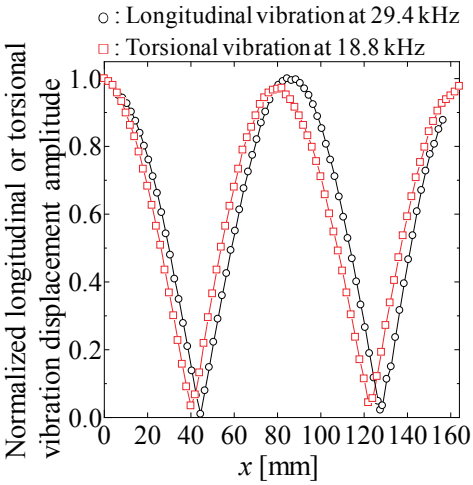

Fig. 3 Vibration distribution.

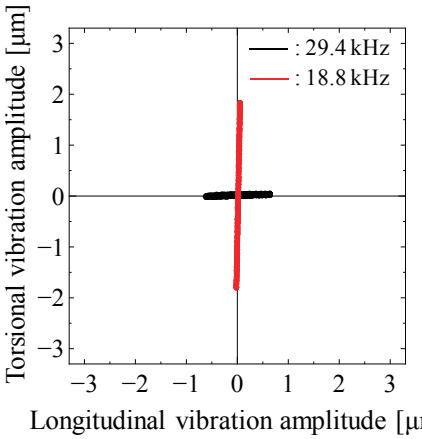

Fig. 4 Vibration locus for one driving frequency.

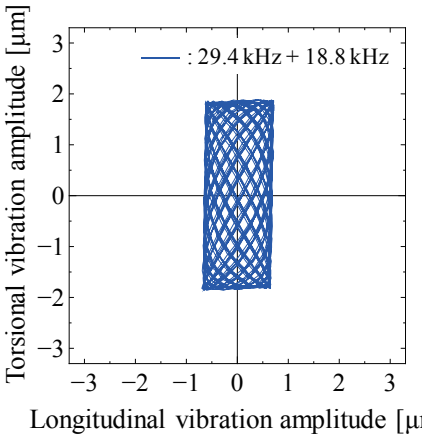

Fig. 5 Vibration locus
for two driving frequencies.